J Solid State Electrochem (2012) 16:2523–2532
DOI 10.1007/s10008-011-1556-8

ORIGINAL PAPER

Improved performances of oxygen potentiometric sensor by electrochemical activation

ChaoYang Xia · XuChen Lu · Yan Yan · TiZhuang Wang · ZhiMin Zhang · SuPing Yang

Received: 13 May 2011 / Revised: 9 August 2011 / Accepted: 12 September 2011 / Published online: 16 February 2012

Abstract It is shown that the performances of the oxygen potentiometric sensor can be remarkably improved by electrochemical activation. The electrochemical activation were carried out by firstly employing the oxygen potentiometric sensor as a fuel cell (H_2 vs. O_2), and then running the fuel cell at a low discharge voltage for some time. This activation effect was valid for sensors domestically prepared under different conditions. On the basis of the literature reports and the experimental observations, the possible reasons for the electrochemical activation have been analyzed. The decrease of the concentration of the oxygen ion (oxide) species at the electrode and the decrease of the electrolyte contribution to the total impedance seemed to be the main reasons that have led to the remarkable improvement of the performances of the oxygen potentiometric sensor after the electrochemical activation.

Keywords Oxygen potentiometric sensor · Electrochemical activation · Performance · Oxygen ion (oxide) species · Electrolyte contribution

Introduction

Potentiometric electrochemical oxygen sensors are commonly used in a variety of applications including internal combustion engines, process control, industrial boilers, and metallurgical heat treatment furnaces [1–3]. A typical oxygen potentiometric sensor consists of an oxygen ion conducting solid electrolyte, usually yttria-stabilized zirconia (YSZ), and two electrodes, such as porous Pt, deposited on the two sides of the electrolyte. When the two electrodes are exposed to two different oxygen partial pressures, the sensor develops an electromotive force (EMF) [3]. If the partial pressure of oxygen at the reference electrode is P_r and that at the sensing electrode is P_w, the generated EMF is given by the Nernst equation:

$$E = \frac{RT}{4F} \ln\left(\frac{P_w}{P_r}\right) \quad (1)$$

Where R is the gas constant, T is the temperature in Kelvin, and F is the Faraday's constant.

Presently, the researches about oxygen potentiometric sensors are mainly focused on two fields: reducing sensor's operation temperature or improving sensor's response rate. The high operation temperature of the oxygen potentiometric sensor is often considered to be related with the low oxygen ion conductivity of the electrolyte at temperatures lower than 600 °C and also due to slow electrode kinetics [3–5]; and the response rate of the oxygen potentiometric sensor is determined by the factors such as double-layer capacitance of the Pt/YSZ interface, material and microstructure of the sensing electrode, conductivity and material of the electrolyte, and electrode reversibility [6, 7].

In order to improve the performances of oxygen potentiometric sensor, many efforts have been carried out: introduction of the electrolytes with high conductivities [5, 8–10] and development of the new materials for sensor's sensing electrode [4, 6, 11, 12]. Compared with some new electrode or electrolyte materials which exhibit excellent catalytic

C. Xia · Z. Zhang · S. Yang
Graduate University of Chinese Academy of Sciences, Beijing 100190, China

X. Lu (✉) · Y. Yan · T. Wang
State Key Laboratory of Complex Systems, Institute of Process Engineering, Chinese Academy of Sciences(CAS), Beijing 100190, China
e-mail: xclu@home.ipe.ac.cn

activity for oxygen reduction, one obvious advantage of the Pt electrode deposited onto the YSZ electrolyte is its expected chemical inertness [13]. This means that employing Pt metal as the starting material to fabricate the sensing electrode has the advantage of extending the lifetime of the oxygen potentiometric sensor. Therefore, until today, the popularly used oxygen potentiometric sensor is still employing Pt as electrode material, and YSZ as the electrolyte.

In addition, surface treatments have also been proposed to reduce the operating temperature of the oxygen potentiometric sensor. HF treatment of stabilized zirconia [14] and a pretreatment with water vapor of LaF_3-based oxygen sensors [15] exhibited good performance at low temperature. However, none of these attempts seem to be sufficiently attractive for industrial production.

In this paper, we show that performances of the oxygen potentiometric sensor can be remarkably improved by firstly employing the sensor as a fuel cell, and then running the fuel cell at a low discharge voltage. The electrochemical activation can substantially reduce sensor's operating temperature, and also can improve sensor's response rate over the operating temperature range from 400 to 700 °C. This promotion effect may be ascribed to the decrease of the concentration of the oxygen ion (oxide) species at the electrode and the decrease of the electrolyte contribution to sensor's total impedance.

Experimental

Sensor fabrication

All prepared sensors employed Pt as the electrode catalyst, and YSZ as the electrolyte. Pt paste (Aldrich), H_2PtCl_6•$6H_2O$ (Beijing Chemical Company, China), the mixture of Pt catalyst (Aldrich, 100 nm) and YSZ sample (Tosch, TZ-8YS, Japan) or the mixture of the Pt catalyst (Aldrich, 100 nm) and graphite (Shanghai YiFan Graphite Company, China) were used as the starting material to prepare the electrodes, and the YSZ samples (Tosch, Japan) with different Y_2O_3 content were used as the electrolytes.

The detailed preparation processes of the electrodes listed in Table 1 are as follows:

1. Pure Pt electrode prepared by Pt paste
   The Pt paste was coated onto the surface of the YSZ tube (40 mm length and 6 mm inner diameter, shown in Fig. 1) or the YSZ pellet (10 mm diameter, 1 mm thickness). After being sintered at 500 °C for 2 h, and then at a high temperature (900 to 1,500 °C) for 2 h, the pure Pt electrode can be prepared.
2. Pure Pt electrode prepared by H_2PtCl_6•$6H_2O$
   The H_2PtCl_6•$6H_2O$ powder was solved into terpilenol (Beijing Chemical Company, China), then some amount

Table 1 Promotion effects for all sensors prepared under different conditions or with different materials and methods

Sample				Response time (s) at 550 °C		Minimum operation temperature (°C)	
No.	Sensing electrode	Electrolyte	Reference electrode	Original	After activation	Original	After activation
1#	Pt paste, sintered at 900 °C	YSZ, TZ-8YS, tube	Pt paste, sintered at 900 °C	15.8	3.1	590	510
2#	Pt paste, sintered at 1,100 °C	YSZ, TZ-8YS, tube	Pt paste, sintered at 1,100 °C	26.8	7.7	610	530
3#	Pt paste, sintered at 1,500 °C	YSZ, TZ-8YS, tube	Pt paste, sintered at 1,500 °C	24.4	9.6	610	540
4#	Decomposition of H_2PtCl_6	YSZ, TZ-8YS, tube	Pt paste, sintered at 900 °C	13.6	2.5	580	490
5#	Pt paste+graphite	YSZ, TZ-8YS, tube	Pt paste	9.8	3.5	550	460
6#	Pt paste+YSZ	YSZ, TZ-8YS, tube	Pt paste	7.3	1.6	490	410
7#	Pt paste	YSZ, TZ-8YS, tube	Pt paste+graphite	14.7	6.7	590	510
8#	Pt paste	YSZ, TZ-8YS, tube	Pt paste+YSZ	15.2	5.3	590	510
9#	Pt paste	YSZ, TZ-5YS, tube	Pt paste	17.8	7.2	620	540
10#	Pt paste, sintered at 900 °C	YSZ, TZ-8YS,pellet	Pt paste, sintered at 900 °C	6.8	1.8	590	510
11#	Decomposition of H_2PtCl_6	YSZ,TZ-8YS,pellet	Pt paste, sintered at 900 °C	5.7	1.3	580	490
12#	Pt paste+graphite	YSZ, TZ-8YS,pellet	Pt paste, sintered at 900 °C	4.3	1.1	550	450
13#	Pt paste+YSZ	YSZ, TZ-8YS,pellet	Pt paste, sintered at 900 °C	3.8	0.9	500	410

The detailed activation process is that employing the sensor as a fuel cell, and then discharging the fuel cell at 0.1 V, 900 °C for about 2 h .The measurements of sensors' performances were carried out with air at the reference electrode and N_2–O_2 mixture at the sensing electrode, and the experimental volume flow rate is about 5–20 $cm^3\ s^{-1}$. The response time values were obtained by changing the oxygen content from 1% to 21%

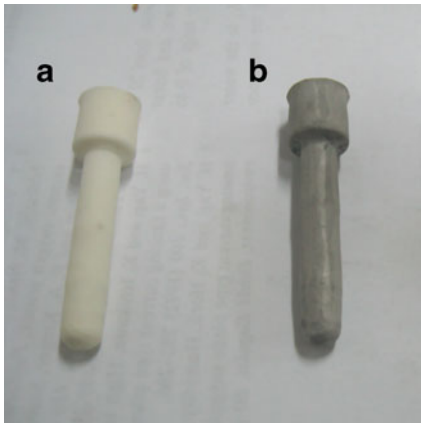

Fig. 1 Typical images of the YSZ tube (**a**) and the YSZ tube coated with the electrodes (**b**)

of Methyl cellulose (Beijing Chemical Company, China) was added into the mixture to prepare a paste. The prepared paste was coated onto the surface of the YSZ tube (40 mm length and 6 mm inner diameter, shown in Fig. 1) or the YSZ pellet (10 mm diameter, 1 mm thickness), and then sintered at 900 °C for about 2 h. The coating and sintering procedures were repeated several times until the electronic resistance between the arbitrary two points on the electrode surface was lower than 1.0 Ω.

3. Pure Pt electrode prepared by the mixture of the Pt catalyst and graphite

   Sixty weight percent of pure Pt catalysts, 8 wt.% of graphite powder, 30 wt.% of polyvinyl alcohol solution (2% in distilled water), and 2 wt.% of glycerol were weighed and mixed to prepare a paste; then, the paste was coated onto the surface of the YSZ tube (40 mm length and 6 mm inner diameter, shown in Fig. 1) or the YSZ pellet (10 mm diameter, 1 mm thickness); after being sintered at 500 °C for 2 h, and then at 1,200 °C for 2 h, the pure Pt electrode can be prepared.

4. Pt–YSZ composite electrode

   The composite electrodes were made using a paste composed of 55 wt.% of Pt, 13 wt.% YSZ, 30 wt.% of polyvinyl alcohol solution (2% in distilled water), and 2 wt.% of glycerol. The paste was then deposited onto the surface of the YSZ tube (40 mm length and 6 mm inner diameter, shown in Fig. 1) or the YSZ pellet (10 mm diameter, 1 mm thickness). After being sintered at 500 °C for 2 h, and then at 1,300 °C for 2 h, the composite electrodes can be prepared. In order to eliminate the influences of the poor electronic conductivities of the Pt–YSZ composites onto the sensing performances, a thin layer prepared by pure Pt catalysts (Aldrich, 100 nm) was deposited onto the Pt–YSZ composite. The deposition process of the thin Pt layer was similar to that of the Pt–YSZ composite electrode: 68 wt.% of pure Pt catalysts, 30 wt.% of polyvinyl alcohol solution (2% in distilled water), and 2 wt.% of glycerol were weighed and mixed to prepare a paste; then, the paste was coated onto the surface of the Pt–YSZ composite; after being sintered at 500 °C for 2 h, and then at 900 °C for 2 h, the thin Pt layer can be prepared.

   Typical image of the YSZ tube coated with electrodes is also shown in Fig. 1. In our experimental, the self-made sensors are all without shield cover.

Electrochemical activation

The equivalent wiring diagram of the implemented activation process is shown in Fig. 2. All the prepared sensors were slowly heated to 700 °C with air at both electrodes and left at this temperature for about 72 h. The sensors were then heated to 800 or 900 °C, and acted as a fuel cell by feeding H_2 and O_2 into the reference electrode and the sensing electrode, respectively. The electrochemical activations were carried out by running the fuel cells at a low voltage, typically 0.1 V, for about 2 h. After the electrochemical activation, the sensors were cooled down to 700 °C at a rate of 2 °C/min with air at both electrodes and left at this temperature for about 12 h.

Electrical measurements

Measurements of sensing performances

The schematic drawing of the measuring setup of sensors' performances is shown in Fig. 3. The oxygen potentiometric sensors were mounted in a furnace, parallel to the gas flow direction. Gas mixtures of controlled gas concentration were applied to the sensors. Gas composition changes were produced by activating solenoid devices that switched alternate gas streams through the furnace and past the sensor. Solenoids were located in the gas stream some 300 cm before the sensor. The solenoid switching time was 0.025–0.050 s. Since the time delay between P_{O2} switch and transport to the sensor is difficult to calculate accurately from the experimental curves, in order to eliminate the influence of the delay time of the gas composition on the response time measurements, we employed Eq. 2 to define the response time.

$$t_\tau = t_{0.95} - t_{0.05} \tag{2}$$

Here, $t_{0.95}$ and $t_{0.05}$ are the times at which the output voltage of the oxygen potentiometric sensor achieves 95% stable voltage and 5% stable voltage, respectively.

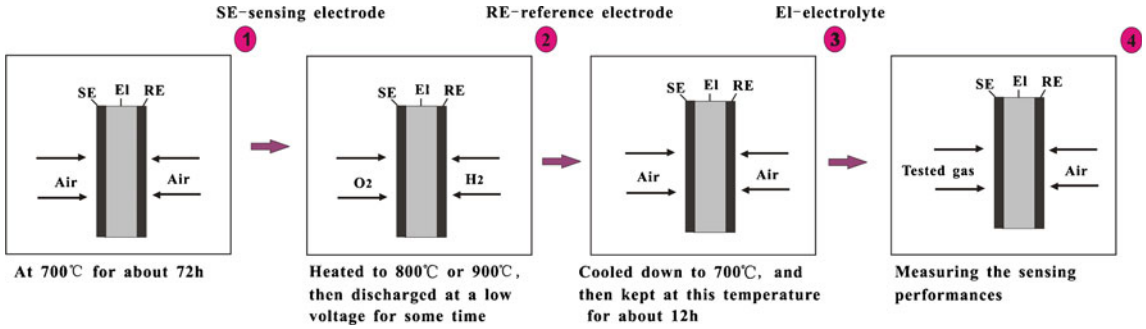

Fig. 2 The equivalent wiring diagram of the implemented activation process

Impedance measurements

Impedance measurements were carried out by an Electrochemical Analysis Meter (CHI614D, manufactured by Hewlett-Packard, USA), and the frequency range was from 10^5 Hz to 0.01 Hz with 10 mV ac signal amplitude at equilibrium potential. Each measurement was repeated twice and the results were in good agreement with each other. The electrode polarization resistance R and the double-layer or constant phase element (Q) values were estimated by fitting the experimental data to the appropriate equivalent circuits.

Results and discussions

Electrochemical activation for oxygen potentiometric sensor

In published works, the oxygen potentiometric sensors often performed with no pre-treatments [3–12, 14, 15]. However, we found that the performances of oxygen potentiometric sensor can be remarkably improved by electrochemical activation. Figure 4 shows the promotion effects on EMF response of the oxygen potentiometric sensor. The electrochemical treatments were carried out by firstly employing the oxygen potentiometric sensor as a fuel cell (H_2 vs. O_2), and then running the fuel cell at about 0.1 V for 2 h. About 12 h after the electrochemical activation, the EMF response curves were measured at 500 °C by feeding a mixture of CO+Air into the sensing electrode, and air into the reference electrode. In Fig. 4, the parameter λ is a signal on how close the mixture Air/CO to stoichiometric conditions. λ is defined as [16]:

$$\lambda = \frac{(V_{air}/V_{CO})_{(actual)}}{(V_{air}/V_{CO})_{(stoichiometric)}} \quad (3)$$

Here, V_{air} is the volume of air in the gas mixture, and V_{CO} is the volume of CO in the gas mixture. Before the electrochemical treatments, the size of the response is far smaller than expected from thermodynamic calculations. However, the situation can be much improved by employing the electrochemical activation. As shown in Fig. 4, after the electrochemical activation, a smooth rise in EMF is observed, and the EMF value at the lean side approaches the theoretical value.

The promotion effects of the electrochemical activation onto sensors' EMF response can be observed more clearly in EMF vs. temperature curves. Figure 5 shows sensor's EMF vs. temperature curves before and after the electrochemical activation. The measurement temperature was ranged from 300 to 700 °C for one representative gas composition, similar behavior to that reported in Fig. 5 was observed for other N_2–O_2 gas mixtures. In Fig. 5, the solid lines represent the theoretical values calculated from Nernst's equation, the close symbols represent the measured values. According to the figure, the electrochemical treatment can reduce sensor's operation temperature from about 590 °C to about 510 °C.

Figure 6 shows the influences of the electrochemical activation onto the sensor's response time. Before the electrochemical activation, the oxygen potentiometric sensor exhibits a 15-s response time at 550 °C, while after the electrochemical activation, sensor's response time was reduced to be about 5 s at 550 °C.

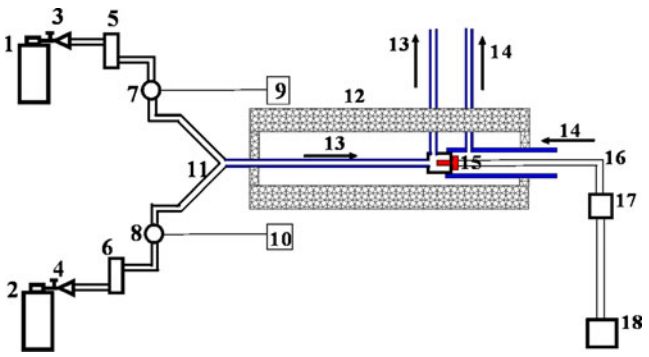

Fig. 3 The schematic drawing of the measuring setup of sensors' performances. *1*, *2* gas cylinders; *3*, *4* globe valves; *5*, *6* gas flow meters; *7*, *8* solenoid valves; *9*, *10* controllers of the solenoid valves; *11* gas pipe; *12* furnace; *13* tested gas; *14* reference gas; *15* oxygen sensor; *16* metal wire; *17* signal detection device; *18* computer

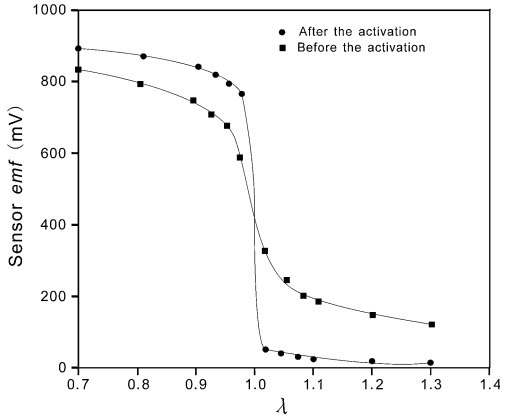

Fig. 4 EMF responses of the oxygen potentiometric sensor at 500 °C before and after the electrochemical activation, measured with air at the reference electrode and air–CO mixture at the sensing electrode. The experimental volume flow rate is about 5–20 cm^3 s^{-1}. The detailed activation process is that employing the sensor as a fuel cell, and then discharging the fuel cell at 0.1 V, 900 °C for about 2 h

Table 1 shows the promotion effects for all sensors prepared under different conditions or with different materials and methods. These sensors included the variations of the sensing electrodes in sintering condition, materials, and microstructure. All the sensors show the promotion effects in the operation temperature and the response rate. It proves that the promotion effects of the electrochemical activation are universal for oxygen potentiometric sensors employing Pt as catalyst and YSZ as electrolyte.

Impedance changes caused by the electrochemical activation

To get an insight into the changes of sensors' performances during the electrochemical activation, the impedances of the

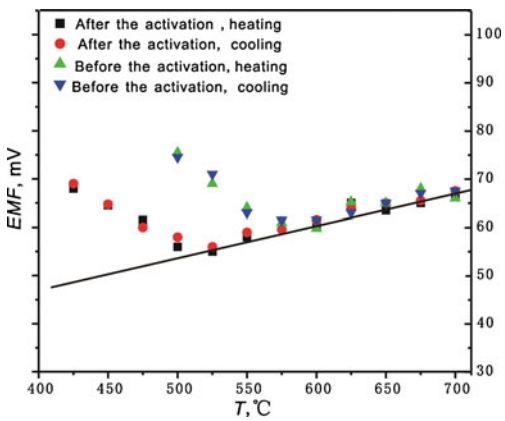

Fig. 5 EMF versus temperature plots for oxygen potentiometric sensor before and after the electrochemical activation, measured with air at the reference electrode and N_2–O_2 mixture at the sensing electrode. The experimental volume flow rate is about 5–20 cm^3 s^{-1}. The detailed activation process is that employing the sensor as a fuel cell, and then discharging the fuel cell at 0.1 V, 900 °C for about 2 h

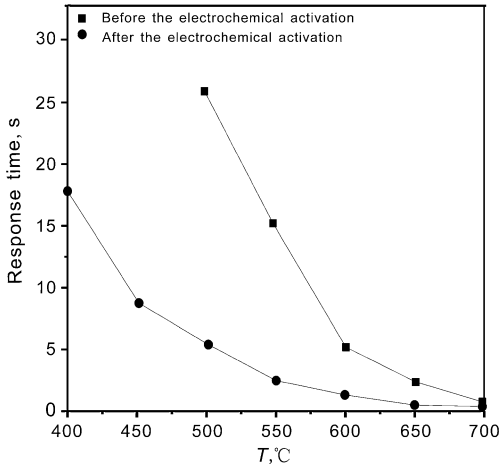

Fig. 6 Response time versus temperature plots for oxygen potentiometric sensor before and after the electrochemical activation, measured with air at the reference electrode and N_2–O_2 mixture (1% O_2 to 21% O_2) at the sensing electrode. The experimental volume flow rate is about 5–20 cm^3 s^{-1}. The detailed activation process is that employing the sensor as a fuel cell, and then discharging the fuel cell at 0.1 V, 900 °C for about 2 h. The response time measurements were carried out 12 h after the electrochemical activation

sensors were measured before and after the electrochemical treatment, respectively. The measured AC impedance spectra are shown in Fig. 7. These Nyquist plots can be approximately interpreted by an equivalent circuit shown in Fig. 8. In Fig. 8, element R_0 could be used to represent the total electrolyte contribution to the impedance [17]. The element R_p Q corresponds to the semicircular arc in the Nyquist plot, in relation to the electron transfer at the electrode. R_p represents the interfacial resistance, Q is a constant phase element [with impedance $Z_Q=1/Q(iw)^n$].

The corresponding impedances of the sensors obtained from Fig. 7 are summarized in Table 2. It can be seen that for all sensors, the values of R_0 and R_p decreased after the electrochemical activation.

Optimization of the electrochemical activation

As the sensor was employed as a fuel cell, applying a small dc bias onto the cell changed the values of the interfacial resistance (R_p), but after switching off the voltage, no promotion effects on sensor's performances and interfacial resistances can be observed. However, if the magnitude of the voltage increased beyond this "reversible regime," drastic changes can be observed (as shown in Table 3).

The influences of the discharge voltage and the temperature onto the promotion effects of the electrochemical activation were measured. The measurements were carried out 12 h after the electrochemical activation, and the results are shown in Table 4. It can be seen that as the fuel cell discharged at 0.3 V, 800 °C, there were no promotion

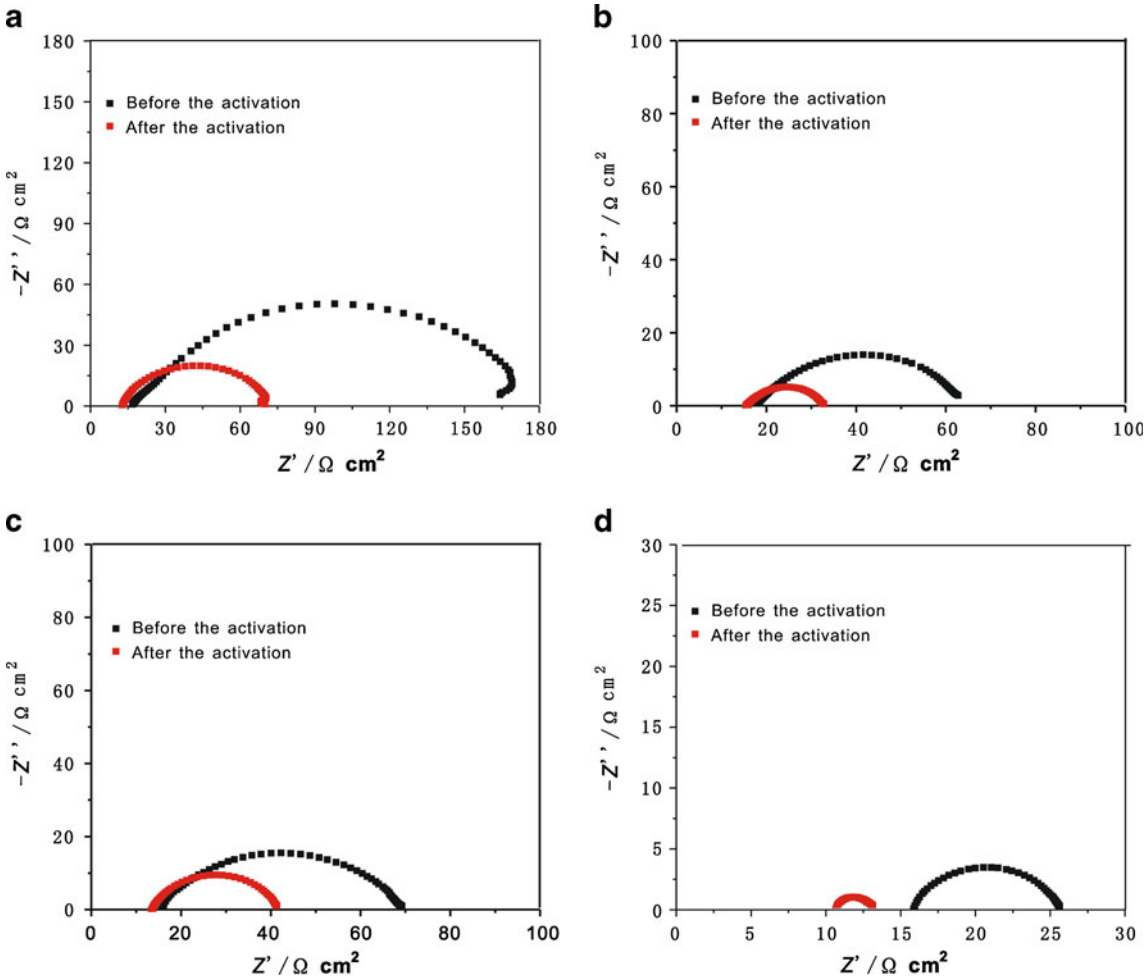

Fig. 7 AC impedance spectra of the oxygen potentiometric sensors before and after the electrochemical activation, measured with air at both electrodes at 700 °C. **a** 1# sensor, **b** 2# sensor, **c** 3# sensor, **d** 4# sensor. The detailed activation process is that employing the sensor as a fuel cell, and then discharging the fuel cell at 0.1 V, 900 °C for about 2 h. The impedance measurements were carried out 12 h after the electrochemical activation

effects onto sensor's operation temperature and response rate; while when the discharge voltage was 0.1 V at 800 °C, obvious promotion effect can be observed. As the temperature increased from 800 to 900 °C, the maximum discharge voltage at which the electrochemical activation can apply obvious promotion effects onto the sensors also increased. However, too high temperature is not beneficial for the improvement of sensors' performances. For example, after activated at 1,100 °C, sensors' performances decreased as compared with the initial state. This may be due to the fact that at the high temperature, platinum particles are more likely to coarsen and crystallize, which would result in a decrease of the three phase contact boundary and an increase in the electrode resistance [4]. The appropriate discharge voltage for electrochemical treatment seems to be ≤0.3 V at 900 °C, and ≤0.1 V at 800 °C.

The length of the time interval during which the electrochemical treatment is applied to the sample also has a strong influence onto the effect of activation. Figure 9 shows the effect of activation time ranging from 5 min to 140 min onto sensor's interfacial resistance. As the activation time increased, the interfacial resistance (R_p) of the sensor firstly decreased with time; but after an enough long time, it achieved a stable value. According to the experimental results, the time interval of 2 h is appropriate for the electrochemical activation.

In our experimental, we also found that the activated state of the sensor, however, was not stable on large time scale. If the sensors were kept at high temperature, the promotion effects seemed to decay with time, but sensors'

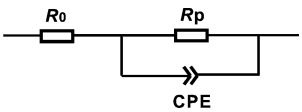

Fig. 8 The equivalent circuit used for interpreting the Nyquist plots

Table 2 The impedances of the sensors measured before and after the electrochemical treatment, measured at 700 °C with air at both electrodes

Sample				R_0 (Ω cm^2)		R_p (Ω cm^2)	
No.	Sensing electrode	Electrolyte	Reference electrode	Original	After activation	Original	After activation
1#	Pt paste	YSZ	Pt paste	16.3	13.6	153	56.5
2#	Decomposition of H_2PtCl_6	YSZ	Pt paste	18.2	15.8	45	18.6
3#	Pt paste+graphite	YSZ	Pt paste	15.4	13.1	56	27.5
4#	Pt paste+YSZ	YSZ	Pt paste	16.8	10.8	10.2	2.7

The detailed activation process is that employing the sensor as a fuel cell, and then discharging the fuel cell at 0.1 V, 900 °C for about 2 h

performances would not recover to the initial states and were still better than those before the activation. This "relaxation" behavior has been further investigated with AC impedance measurement over 7 h, the measurement results are shown in Fig. 10. After enough long time, the interfacial resistance seems to achieve a stable value, which is still lower than the initial value before the electrochemical activation.

According to above observations, we can conclude that during the electrochemical activation, there were two kinds of promotion effects applied onto the sensors, one is reversible, which has led to the "relaxation" behavior of the sensors after the electrochemical activation; while the other is irreversible and beneficial for the permanent improvement of sensors' performances.

Possible reasons for the electrochemical activation

For metal and ceramic electrodes, promotion effects of the electrochemical activation have often been observed [18–27]. Summarizing the literature reports and the experimental observations presented above, the following two factors can be accounted for the promotion effects of the electrochemical activation.

Decrease of the concentration of the oxygen ion (oxide) species

Although the electrochemical reactions occurring in an $O_{2(g)}$, Pt/YSZ system are still under discussion due to the complexity of the system, the occurrence of oxygen ion (oxide) species has been reported by many literatures [21–23, 25] . The oxygen ion (oxide) species are also present at the three-phase boundaries (TPB). Since the TPBs are the necessary sites for oxygen charge transfer [13], the presence of oxygen ion (oxide) species will result in blockage of effective number of the electrochemical reaction site, and then lead to increase of the interfacial resistance and reduction of the electrode capacitance.

According to Sridhar's reports [22, 23], in oxygen-containing atmosphere it is likely that the oxygen in the gas phase equilibrates with the electrode and then results in the formation of various oxygen ion (oxide) species, which effectively reduces the concentration of charge-transfer sites and increases the impedance response:

$$O_{2(g)} + 2(Pt)_n \rightleftarrows 2(Pt)_nO \quad (4)$$

The oxygen ion (oxide) species include all types of species present at electrode from weakly adsorbed oxygen

Table 3 Influences of the bias voltage onto the changes of the interfacial resistances

No.	Bias voltage (V)	Discharge voltage (V)	R_0 (Ω cm^2)		R_p (Ω cm^2)	
			Before the activation	After the activation	Before the activation	After the activation
1#	0.15	0.8	19.8	19.8	65	65
2#	0.35	0.6	16.5	16.5	58	58
3#	0.55	0.4	17.6	17.8	71	71
4#	0.65	0.3	15.7	15.7	49	49
5#	0.75	0.2	14.8	13.9	51	43
6#	0.85	0.1	16.5	14.1	61	39

The detailed process is that employing the sensor as a fuel cell and then applying a bias voltage onto the fuel cell for about 2 h at 800 °C. The open-circuit voltage of the fuel cell is about 0.95 V. The interfacial resistances were measured at 700 °C with air at both electrodes, 12 h after the electrochemical treatment

Table 4 Influences of the discharge voltage and the temperature onto the promotion effects of the electrochemical activation

No.	Parameters of the electrochemical activation		Effect on sensor's performances	
	Discharge voltage (V)	Temperature(°C)	Operation temperature	Response time
1#	0.1	800	↓	↓
2#	0.3	800	—	—
3#	0.5	800	—	—
4#	0.1	900	↓	↓
5#	0.3	900	↓	↓
6#	0.5	900	—	—
7#	0.1	1,100	↑	↑
8#	0.3	1,100	↑	↑
9#	0.5	1,100	↑	↑

↓ decreasing, ↑ increasing, — no change

atoms to stable oxide. However, the passage of a direct current can alter the oxygen ion (oxide) species according to:

$$(\mathrm{Pt})_n\mathrm{O} + 2\mathrm{e}^- \rightleftarrows n\mathrm{Pt} + \mathrm{O}^{2-} \quad (5)$$

By virtue of Eq. 5, a cathodic current should decrease the oxygen ion (oxide) species concentration at the TPB. Accordingly, the interfacial resistance can be observed to decrease due to the enhancement of the electrochemical reaction sites.

In our experimental, we firstly employed the oxygen potentiometric sensor as a fuel cell, and then run the fuel cell at a low voltage for some time. As the fuel cell was in normal operation, a cathodic current would pass through the sensing electrode. So according to the abovementioned theory, during the electrochemical activation, the oxygen ion (oxide) species concentration at the TPB would decrease, which resulted in the increase of the effective number of the electrochemical reaction site. The increase of the effective number of the electrochemical reaction site is beneficial for enhancement of the electrode activity, as well as sensor's interfacial resistance. So after the electrochemical activation, sensor's operation temperature and response time both can be lowered.

As seen in Fig. 10, after the electrochemical activation, the activated sensor is not in a stable state, it exhibits a "relaxation" behavior. The loosely bonded oxygen O…$(\mathrm{Pt})_n$, that easily re-forms/decays, is mostly likely responsible for this "relaxation" effect [22, 23]. However, after enough long time, sensors' interfacial resistance will not return to its initial value, it seems to achieve a stable value, which is still lower than the initial value before the electrochemical activation. The oxide-like O-$(\mathrm{Pt})_n$ may be one of the possible reasons for this irreversible change [22, 23].

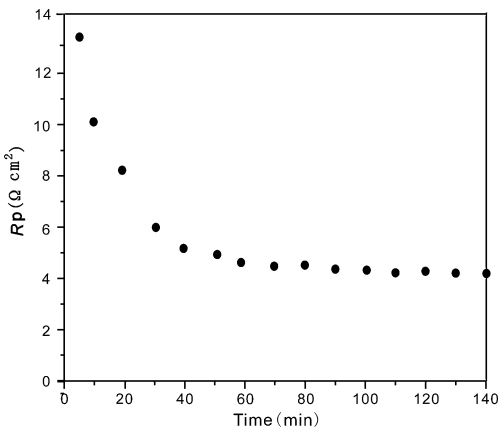

Fig. 9 The effect of the activation time onto sensor's interfacial resistance after the electrochemical activation, measured at 700 °C with air at both electrodes. The detailed activation process is that employing the sensor as a fuel cell, and then discharging the fuel cell at 0.1 V, 900 °C. The impedance measurements were carried out 12 h after the electrochemical activation

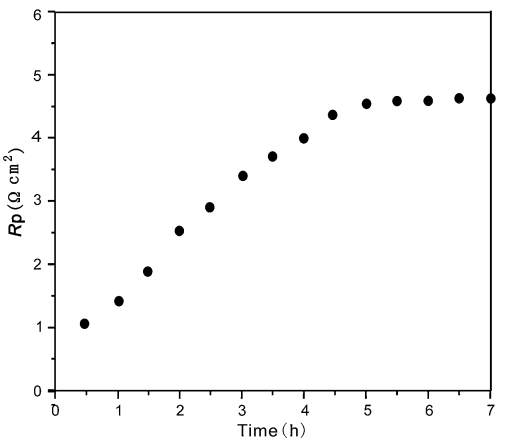

Fig. 10 Relaxation behavior of the interfacial resistance after the electrochemical activation, measured at 700 °C with air at both electrodes. The detailed activation process is that employing the sensor as a fuel cell, and then discharging the fuel cell at 0.1 V, 900 °C for about 2 h. After the electrochemical activation, the sensors were cooled down to 700 °C at a rate of 2 °C/min with air at both electrodes

Decrease of the electrolyte contribution to the total impedance

According to Table 2, after the electrochemical activation, the electrolyte contribution to the total impedance (R_0) decreased. Similar experimental results also can be found in the existed literatures. Nazarpour et al. [26] observed a decrease of the resistance in crystals of the super-ionic YSZ when the crystals are reduced during the application of an electric field. Nazarpour's another paper showed [27] applying an electric field onto the super-ionic YSZ not only can decrease the electrolyte contribution to the total impedance, but also can enhance the electrolyte's thermal stability.

PaiVerneker et al. [28] calculated that the YSZ bandgap energy increases from 4.23 to 4.96 eV by subjecting the YSZ to a predetermined voltage at 600 °C. They explained that during the electrical treatment, the density of singly occupied vacancies would be increased. Next, these vacancies form a well-known complex with Y^{3+} (or Al^{3+}) which is called F_A centers [29]. Electrical treatment generates F_A centers which the ground state of these defect pairs lies in the valence band. Now, considering that each Y atom produces a singly occupied oxygen vacancy, therefore up to half of Y^{3+} are close to an oxygen vacancy; hence, large concentration of F_A centers could be found within the YSZ matrix. PaiVerneker et al. [28] showed that the interaction within F_A centers generates an excited state; the energy of this state could be controlled by voltage and time of electrical treatment.

Essentially, the electric field causes the crystals of the super-ionic YSZ to lose oxygen and the applied temperature accelerates this loss. The loss of the oxygen results in the removal of O^{2-} ions from the lattice, each of which is replaced by two electrons and a vacancy which results in a doubly occupied vacancy. As the concentration of doubly occupied vacancies increased, the mean energy of this band is raised due to lattice relaxation. Eventually, part of this band decays into valence band which results in its new energy states [26]. Therefore, applying an electric field through the YSZ ionic conductor at certain conditions could enhance the ionic conductivity of the component.

The experimental data in Table 3 shows that if the discharge voltage of the electrochemical activation is appropriate, R_0 will decrease and will not return to the initial values after the electrochemical activation. This means that the decrease of the electrolyte contribution to the total impedance will result in an irreversible change of the sensors' performances.

Conclusions

It is shown that the performances of the oxygen potentiometric sensor can be remarkably improved by electrochemical activation. The electrochemical activation were carried out by firstly employing the oxygen potentiometric sensor as a fuel cell (H_2 vs. O_2), and then running the fuel cell at a low discharge voltage for some time.

The promotion effects of the electrochemical activation are dependent on the magnitude of the discharge voltage and activation time. After an initial time-dependent change, the performances of the activated oxygen potentiometric sensor evolve towards a new steady state different from the initial steady state. This transient part of the change has been further investigated with AC impedance measurement. The measurement results show that there are two kinds of promotion effects applied onto the sensors, one is reversible, which have led to the "relaxation" behavior of the sensors after the electrochemical activation, while the other is irreversible and beneficial for the permanent improvement of the performances of the sensors.

On the basis of the literature reports and the experimental observations, the possible reasons for the electrochemical activation have been analyzed. The decrease of concentration of the oxygen ion (oxide) species at the electrode and the decrease of the electrolyte contribution to the total impedance seemed to be the main reasons that have led to the remarkable improvement of the performances of the oxygen potentiometric sensor after the electrochemical activation.

References

1. Williams DE, McGeehin P (1984) Solid state gas sensors and monitors. Electrochem 9:246–290
2. Vitterm G, Foster P, Lahlou M, Gutierrez Monreal FJ (1983) Use of an oxygen mini-gauge for monitoring domestic and medium sized boilers. Solid State Ionics 9–10:1273–1276
3. Radhakrishnan R, Virkar AV, Singhal SC, Dunham GC, Marina OA (2005) Design, fabrication and characterization of a miniaturized series-connected potentiometric oxygen sensor. Sensor Actuator B Chem 105:312–321
4. Badwal SPS, Ciacchi FT, Haylock JW (1988) Nernstian behavior of zirconia oxygen sensors incorporating composite electrodes. J Appl Electrochem 18:232–239
5. Kleitz M, Iharada T, Abraham F, Mairesse G, Fouletier J (1993) Electrode material for zirconia working at temperatures lower than 500 K. Sensor Actuator B Chem 13–14:27–30
6. Maskell W (1987) Inorganic solid state chemically sensitive devices: electrochemical oxygen gas sensors. J Phys E Sci Instrum 20:1156–1168
7. Winnubst AJA, Scharenborg AHA, Burggraaf AJ (1985) Response behavior of oxygen sensing solid electrolytes. J Appl Electrochem 15:139–144
8. Alberti G, Carbone A, Palombari R (2002) Oxygen potentiometric sensors based on thermally stable solid state proton conductors: a preliminary investigation in the temperature range 15–200 °C. Sensor Actuator B Chem 86:150–154
9. Siebert E, Fouletier J, Vilminot S (1983) Characteristics of an oxygen gauge at temperature lower than 200 °C. Solid State Ionics 9–10:1291–1294

10. Yamazoe N, Hisamoto J, Miura N (1987) Potentiometric solid state oxygen sensor using lanthanum fluoride operative at room temperature. Sensor Actuator B Chem 12:415–423
11. Badwal SPS, Ciacchi FT (1986) Performances of zirconia membrane oxygen sensors at low temperature with nonstoichiometric oxide electrodes. J Appl Electrochem 16:28–40
12. Salgado JR, Fabry P (2002) Feasibility of potentiometric oxygen gas sensor based on perovskite and sodium titanate measuring electrode. Sensor Actuator B Chem 82:34–39
13. Nielsen J, Jacobsen T (2007) Three-phase-boundary dynamics at Pt/YSZ micro-electrodes. Solid State Ionics 178:1001–1009
14. Obayashi H, Okamoto H (1981) Low-temperature performance of fluoride-ion-treated ZrO_2 oxygen sensor. Solid State Ionics 3–4:631–634
15. Miura N, Hisamoto J, Yamazoe N, Kuwata S, Salardenne J (1989) Solid state oxygen sensor using sputtered LaF3 film. Sensor Actuator B Chem 16:301–310
16. Gandara CL, Ramos FM, Cirera A (2009) YSZ-based oxygen sensors and the use of nanomaterials: a review from classical models to current trends. J Sens. doi:10.1155/2009/258489
17. Wang T, Robert FN, Richard ES (2001) A study of factors that influence zirconia/platinum interfacial impedance using equivalent circuit analysis. Sensor Actuator B Chem 77:132–138
18. Baumann FS, Fleig J, Konuma M, Starke U, Habermeier HU, Maier J (2005) Strong performance improvement of $La_{0.6}Sr_{0.4}Co_{0.8}Fe_{0.2}O_{3-\delta}$ SOFC cathode by electrochemical activation. J Eletrochem Soc 152:A2074–A2079
19. Jiang SP, Love JG (2001) Origin of the initial polarization behavior of Sr-doped $LaMO_3$ for O_2 reduction in solid oxide fuel cells. Solid State Ionics 138:183–190
20. Jiang SP, Love JG (2003) Observation of structural change induced by cathodic polarization on (La, Sr) MnO3 electrodes of solid oxide fuel cells. Solid State Ionics 158:45–53
21. Jacobsen T, Christiansen BZ, Bay L, Jorgensen MJ (2001) Hysteresis in the solid oxide fuel cell cathode reaction. Electrochim Acta 46:1019–1024
22. Sridhar S, Stancovski V, Pal UB (1997) Effect of oxygen-containing species on the impedance of the Pt/YSZ interface. Solid State Ionics 100:17–22
23. Sridhar S, Stancovski V, Pal UB (1997) Transient and permanent effects of direct current on oxygen transfer across YSZ-electrode interface. J Electrochem Soc 144:2479–2485
24. Ricoult MB, Adib K, Clair TS, Luerssen B, Gregoratti L, Barinov A (2008) In-situ study of operating SOFC LSM/YSZ cathodes under polarization by photoelectron microscopy. Solid State Ionics 179:891–895
25. Ladas S, Kennou S, Bebelis S, Vayenas CG (1993) Origin of non-faradic electro- chemical modification of catalytic activity. J Phys Chem 97:8845–8848
26. Nazarpour S, Lopez C, Ramos F, Cirera A (2011) Structural and electrical properties of Y-doped zirconia induced by electrical polarization. Solid State Ionics 184:19–22
27. Nazarpour S, Lopez C, Ramos F, Cirera A (2011) An enhancement in thermal stability of alumina doped YSZ by applying an electric field. Mater Sci Eng 528:5400–5408
28. Paivemeker VR, Petelin AN, Crowne FJ, Nagle DC (1989) Color-center-induced band-gap shift in yttria-stabilized zirconia. Phys Rev B 40:8555–8557
29. Subbarao EC, Maiti HS (1984) Solid electrolytes with oxygen ion conduction. Solid State Ionics 11:317–338